

# GCAD: Anomaly Detection in Multivariate Time Series from the Perspective of Granger Causality

Zehao Liu<sup>1</sup>, Mengzhou Gao<sup>1,2</sup>, Pengfei Jiao<sup>1,2,3\*</sup>

<sup>1</sup>Zhuoyue Honors College, Hangzhou Dianzi University, China

<sup>2</sup>School of Cyberspace, Hangzhou Dianzi University, China

<sup>3</sup>Data Security Governance Zhejiang Engineering Research Center, Hangzhou Dianzi University, China  
{zhaoliu, mzgao, pjiao}@hdu.edu.cn

## Abstract

Multivariate time series anomaly detection has numerous real-world applications and is being extensively studied. Modeling pairwise correlations between variables is crucial. Existing methods employ learnable graph structures and graph neural networks to explicitly model the spatial dependencies between variables. However, these methods are primarily based on prediction or reconstruction tasks, which can only learn similarity relationships between sequence embeddings and lack interpretability in how graph structures affect time series evolution. In this paper, we designed a framework that models spatial dependencies using interpretable causal relationships and detects anomalies through changes in causal patterns. Specifically, we propose a method to dynamically discover Granger causality using gradients in nonlinear deep predictors and employ a simple sparsification strategy to obtain a Granger causality graph, detecting anomalies from a causal perspective. Experiments on real-world datasets demonstrate that the proposed model achieves more accurate anomaly detection compared to baseline methods.

## Introduction

Time series data are prevalent in the real world. Many industrial systems, such as water supply systems, aerospace, and large server systems, have extensive sensor networks that generate vast amounts of multivariate time series (MTS) data. These systems exhibit complex internal dependencies and nonlinear relationships. With the rapid development in related fields, discovering system anomalies from the large volumes of monitoring data generated by sensors has become an important issue. This is crucial for maintaining the safe operation of systems and reducing economic losses (Tuli, Casale, and Jennings 2022; Zhang et al. 2024).

Capturing inter-series relationships has been proven to effectively enhance the performance of MTS anomaly detection (Zheng et al. 2023; Zamanzadeh Darban et al. 2024). Recently, Graph Neural Networks (GNNs) have shown great potential in time series anomaly detection by effectively capturing spatial dependencies between variables (Chen et al. 2021). Considering that most time series datasets do not provide readily available graphs, many existing methods adaptively learn graph structures, and then use reconstruction or

prediction errors for anomaly detection (Jin et al. 2024). A key problem is that these models only learn the similarity of sequence embedding vectors without exploring the role of the graph structure in the evolution of time series.

In real-world scenarios, anomalies in time series are often accompanied by changes in dependency structures. For example, consider a simple pipeline in a water supply system. Under normal conditions, when water pressure increases at the inflow end, it leads to a corresponding increase at the outflow end. However, if there is a leak in the pipeline, an increase in inflow pressure may no longer result in the expected pressure increase at the outflow end. Therefore, learning interpretable dependency structures with causal relationships can effectively detect anomalies in the evolution patterns of time series. However, there are several key challenges in using causal relationships to detect anomalies:

- Real systems have complex control logic and numerous nonlinear associations, making it difficult to learn interpretable dependency relationships between variables in a data-driven manner.
- The dependency relationships between variables are time-varying, and dynamically capturing dependency patterns in the system and identifying anomalies is a key issue.

Time series causality is a promising tool for modeling spatial dependencies. Granger introduced Granger causality (Granger 1969). The core idea of Granger causality is straightforward: if using the series  $x_i$  does not help reduce the prediction error of another series  $x_j$ , then  $x_i$  does not Granger-cause  $x_j$  (Shojaie and Fox 2022). The original definition of Granger causality was intended for linear systems, but recent studies (Khanna and Tan 2019; Liu et al. 2023; Cheng et al. 2024) have extended Granger causality to nonlinear relationships.

In this paper, we propose a Granger Causality-based multivariate time series Anomaly Detection method (GCAD). To address the first challenge, we combine deep models with Granger causality. Deep networks have powerful modeling capabilities for nonlinear relationships. We leverage this capability to uncover complex causal relationships from black-box deep networks. To tackle the second challenge, we propose using the gradients in nonlinear deep models to dynamically mine causal dependencies. During the training

\*Corresponding author

phase, normal causal patterns are embedded into the deep network. When anomalies occur, the nonlinear deep network will yield significantly deviated causal patterns. Our hypothesis is that when an anomaly occurs, the Granger causality patterns between sequences will change significantly.

Based on the definition (Cheng et al. 2022) of Granger causality, we introduce a channel-separated gradient generator and quantify the Granger causality effect as an integral of deep predictor gradients over the time lag. Our motivation is that the gradients of a network reflect its internal structure to some extent. Utilizing Granger causality discovered from network gradients will help us leverage internal information from black-box models. Discovering Granger causality from the gradient perspective offers many advantages. Deep predictors can automatically learn complex nonlinear relationships between variables. Most importantly, compared to existing Granger causality discovery methods, our approach does not require repeated optimization and parameter adjustment during the testing phase.

Going beyond previous methods, we first train a simple predictor on data without anomalies and then use our proposed gradient-based Granger causality effect quantification method to obtain dynamic spatial dependencies between sequences. To impose sparsity constraints on the causal graph, we use a symmetry-based sparsification method to eliminate bidirectional edges and reduce the impact of sequence similarity on Granger causality effects. It is noteworthy that the output matrix generated by our method contains both spatial dependency information and temporal dependency information. By combining the deviations from these two types of dependencies to compute anomaly scores, our method has achieved excellent results on five real-world benchmark datasets. Our contributions are summarized as follows:

- We propose using the deviation of dynamic Granger causality patterns for time series anomaly detection. To the best of our knowledge, our proposed method is the first research to combine deep models with Granger causality for time series anomaly detection.
- We construct Granger causal graphs using deep model gradients, avoiding frequent online optimization during the testing phase, and propose an effective method for causal graph sparsification.
- Our method achieved state-of-the-art anomaly detection results on most of the five real-world benchmark datasets.

## Related Work

### Multivariate Time Series Anomaly Detection

Multivariate time series anomaly detection is widely applied in the real world. As a classic task in the field of time series analysis, it has received extensive research attention. Early research primarily focused on statistical methods, such as ARIMA (Yu, Jibin, and Jiang 2016), (Keogh, Lin, and Fu 2005) and (Wang et al. 2018). Recently, many deep learning-based methods have been proposed, which effectively capture nonlinear information and are not constrained by the stationarity assumption. These include methods based on Convolutional Neural Networks (CNN) (Munir et al. 2018;

Zhang et al. 2019; Tayeh et al. 2022) and Long Short-Term Memory(LSTM) networks (Hundman et al. 2018), among others.

With the development of autoencoders and their variants, many studies have explored using Variational Autoencoders (VAE) (Park, Hoshi, and Kemp 2018; Su et al. 2019) or Generative Adversarial Networks (GAN) (Zhou et al. 2019; Li et al. 2019) for anomaly detection. However, these methods do not explicitly learn the spatial dependencies between sequences, and as pointed out in (Zheng et al. 2023), they fail to fully exploit the dependencies between variable pairs.

Recently, graph neural networks (GNN) have been increasingly applied to the problem of sequence anomaly detection. By modeling sequences as nodes and the correlations between sequences as edges, using a graph data structure and GNNs naturally represents the spatial relationships between variables. A key challenge in applying GNNs to sequence anomaly detection is that the required knowledge of graph structure usually does not inherently exist in time series anomaly detection data (Li et al. 2021). To address this challenge, many studies have explored adaptive graph learning modules, with GDN (Deng and Hooi 2021) being a pioneering work in this area (Jin et al. 2024). GDN calculates the graph structure based on the cosine distance of sequence embeddings. Most graph-based methods (Han and Woo 2022) use GNNs for prediction or reconstruction, but they do not directly apply spatial dependency patterns to anomaly detection.

### Inter-sequence Correlations Modeling

Explicitly modeling spatial dependencies between sequences helps in discovering more complex anomalies. Most GNN-based methods construct static graph structures using randomly initialized embedding vectors to model spatial dependencies. Methods like VGCRN (Chen et al. 2022) and FuSAGNet (Han and Woo 2022) compute dot products between embeddings to generate a similarity matrix used as a graph structure. However, optimization methods based on downstream tasks may not yield stable and meaningful graph structures. Another class of methods leverages self-attention mechanisms for modeling. The reconstruction module of Grelen (Zhang, Zhang, and Tsung 2022) learns to dynamically construct graph structures that adapt to each time point based on the input time series data. However, randomly initialized attention networks may result in learned spatial relationships that lack practical significance (Zhang, Geng, and Han 2024).

Some limited studies (Qiu et al. 2012) have explored using Granger causality to model spatial relationships between sequences, but they are based on simple linear statistical models and cannot capture complex nonlinear dependencies. Other methods (Tank et al. 2021) discover Granger causality from sparse penalized network weights. However, this approach is not suitable for anomaly detection tasks. Because data is input in a streaming fashion, and these methods have to continuously optimize parameters during testing to adapt to dynamic causal relationships, resulting in substantial computational costs.

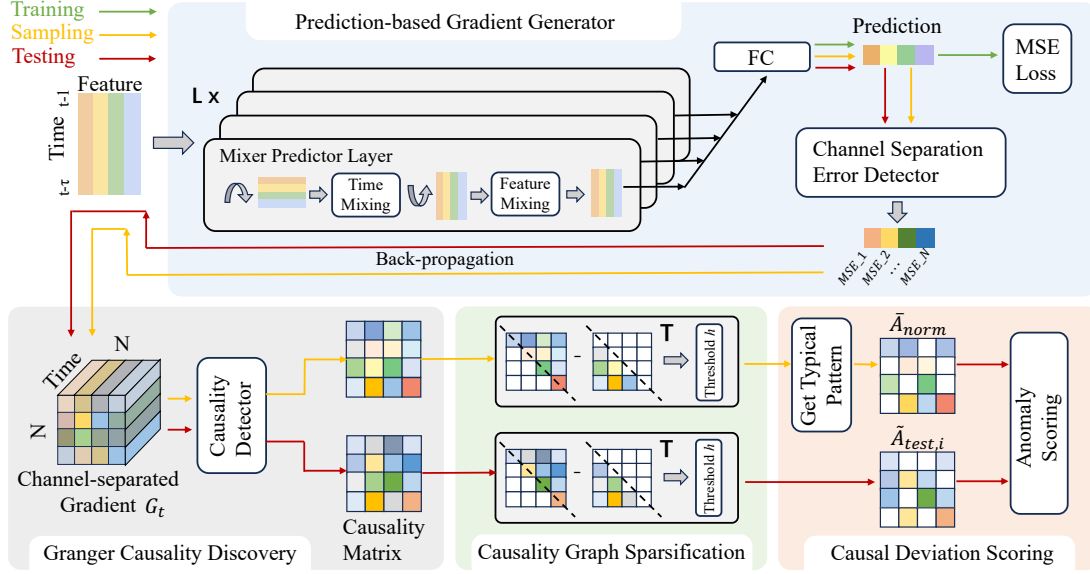


Figure 1: Overall Architecture of GCAD. During the training phase, the gradient generator is trained for the prediction task. In the sampling and testing phases, the gradient information from the training samples and test data within the predictor is used to perform Granger causality discovery, and the causal graphs are obtained through sparsification. Anomaly scores are calculated by measuring the deviation of the causal graphs from the normal pattern.

## Methodology

### Problem Statement

In this paper, we investigate the task of anomaly detection in multivariate time series. Our multivariate time series data are collected from various sensors in a real system, observed at equal intervals over a period of time. The observed time series can be represented as a set of time points:  $\{x_1, x_2, \dots, x_T\}$ , where  $x_t \in \mathbb{R}^N$  denotes the observations from  $N$  sensors at time  $t$ . In the anomaly detection task, the input to the model is a sliding window  $\{x_{t-\tau}, \dots, x_{t-1}, x_t\}$ . The model outputs a Boolean value for each sliding window to determine whether there is an anomaly within that window.

### Overview

Our GCAD framework aims to extract Granger causality relationships among multivariate time series and then identify anomalies from the causal patterns on the test set. It mainly consists of the following four parts:

1. **Prediction-based Gradient Generator:** Utilizes predictive methods to guide training and provides channel-separated gradients during the causality discovery phase.
2. **Granger Causality Discovery:** Dynamically infers Granger causal relationships from the gradients produced by the gradient generator.
3. **Causality Graph Sparsification:** Applies sparsity constraints to the discovered causal relationships to obtain a causality graph matrix.
4. **Causal Deviation Scoring:** Calculates the causal pattern deviation score and integrates temporal information to detect anomalies.

Figure 1 provides an overview of our framework.

### Prediction-based Gradient Generator

The widely studied Mixer predictor (Chen et al. 2023) is used as the gradient generator in our GCAD framework. The predictor consists of  $L$  stacked Mixer Predictor Layers, each containing interleaved temporal mixing and feature mixing MLPs. The temporal mixing MLPs are shared across all  $N$  features, while the feature mixing MLPs are shared across all time steps. The output of each layer is fed through skip connections into a fully connected layer to produce the predictive output.

The input to the predictor is the sliding window  $X_{t-1} = \{x_{t-\tau}, x_{t-\tau+1}, \dots, x_{t-1}\}$ , where  $\tau$  is the maximum time lag considered for Granger causality, and  $X_t \in \mathbb{R}^{N \times \tau}$ . The predictor outputs the prediction for time  $t$ :  $\hat{y}_t = f(X_{t-1})$ . Where  $f$  is the prediction function fitted by the predictor, and  $\hat{y}_t \in \mathbb{R}^N$ . During the training phase, the MSE (Mean Squared Error) loss is used to guide the optimization of predictor parameters:  $L_{train} = MSE(\hat{y}_t, y_t)$ , where  $y_t$  is the ground truth.

During the testing phase, in order to explore the causal relationships between variables, the gradient generator needs to compute pairwise predictor gradients between variables. Therefore, we propose a channel-separated Error detector to generate channel loss  $L_t \in \mathbb{R}^N$ :

$$L_{t,j} = (\hat{y}_{t,j} - y_{t,j})^2, \quad (1)$$

where  $L_{t,j}$  represents the prediction error of sequence  $j$  in the sliding window  $X_t$ . Next, the gradient generator performs backpropagation on each prediction error through the prediction network, obtaining the gradient  $G_{t,j} \in \mathbb{R}^{N \times \tau}$

on  $X_t$ . We compile the complete gradient tensor  $G_t \in \mathbb{R}^{N \times N \times \tau}$  by stacking all the gradients together.

### Granger Causality Discovery

Nonlinear Granger causality is defined from the perspective of the impact of variables on each other’s predictive effects. Our framework reconsiders Granger causality from the perspective of gradients in deep networks. In this paper, we adopt the widely used definition (Cheng et al. 2022) of nonlinear Granger causality:

**Definition 1** *Time series  $i$  Granger-causes  $j$  if and only if there exists  $x'_{t-\tau:t-1,i} \neq x_{t-\tau:t-1,i}$ ,*

$$\begin{aligned} f_j(x_{t-\tau:t-1,1}, \dots, x'_{t-\tau:t-1,i}, \dots, x_{t-\tau:t-1,N}) &\neq \\ f_j(x_{t-\tau:t-1,1}, \dots, x_{t-\tau:t-1,i}, \dots, x_{t-\tau:t-1,N}). \end{aligned} \quad (2)$$

*i.e., the past data points of time series  $i$  influence the prediction of  $x_{t,j}$ .*

Considering this definition from a differential perspective, let  $t' \in (t - \tau : t - 1)$ , and let  $x'_{t',i}$  be a perturbation of  $x_{t',i} \in X_t$ :

$$x'_{t',i} = x_{t',i} + \Delta, \quad (3)$$

where  $\Delta$  is the perturbation. Based on the predictor described in the previous subsection, the following equations can be obtained:

$\hat{y}_{t,j} = f_j(x_{t-\tau:t-1,1}, \dots, x_{t-\tau:t-1,i}, \dots, x_{t-\tau:t-1,N})$ , and  $\hat{y}^*_{t,j} = f_j(x_{t-\tau:t-1,1}, \dots, \{x_{t-\tau,i}, \dots, x'_{t',i}, \dots, x_{t-1,i}\}, \dots, x_{t-\tau:t-1,N})$ . Where  $f_j$  is the function of  $\hat{y}_{t,j}$  with respect to the input in the prediction network. The change in prediction error caused by the perturbation can be transformed into the form of partial derivatives:

$$\lim_{\Delta \rightarrow 0} |L_{t,j} - L^*_{t,j}| = \left| \frac{\partial L_{t,j}}{\partial x_{t',i}} \right| \cdot |\Delta|, \quad (4)$$

where  $L^*_{t,j} = (\hat{y}^*_{t,j} - y_{t,j})^2$ . Granger causality considers the mutual influence of sequences on each other’s predicted values within the maximum time lag. Therefore, we define the quantification of Granger causality as the integral of the absolute values of channel-separated gradients over the time lag:

$$a_{i,j} = \int_{t-\tau}^{t-1} \left| \frac{\partial L_{t,j}}{\partial x_{\phi,i}} \right| P(x_{\phi,i}) dx_{\phi,i}, \quad (5)$$

where  $\phi$  is the time index from  $t - \tau$  to  $t - 1$ . The term  $a_{i,j}$  represents the degree to which sequence  $i$  Granger causes sequence  $j$ , parameterized by a distribution of interest  $P$ . The causality matrix is defined as  $A = \{a_{i,j}\}_{i,j=1}^N$ .

Since predictors composed of deep networks are capable of backpropagation, the prediction function  $f$  is inherently continuous and differentiable. For simplicity, the interest distribution  $P$  can be a uniform distribution. According to Equation 4, when  $a_{i,j} \neq 0$ , it can be concluded that the two predicted values are not equal, i.e.,  $\hat{y}^*_{t,j} \neq \hat{y}_{t,j}$ . Since the inputs corresponding to these two predicted values are  $x'_{t',i}$  and  $x_{t',i}$ , respectively, the differing inputs of sequence  $i$  result in differing outputs of sequence  $j$ . This is consistent with Definition 1, from which it can be inferred that sequence  $i$  Granger-causes sequence  $j$ .

### Causality Graph Sparsification

Unlike similarity or correlation between sequences, causality must be unidirectional. The ideal Granger causality graph is a directed acyclic graph (DAG). However, in nonlinear Granger causality discovery, it is difficult to strictly guarantee the acyclic nature of the causal graph. Existing methods discover nonlinear causality through network weights constrained by sparsity. To adapt to the anomaly detection task, instead of directly constraining the weights, we employ sparsification to address the dynamic Granger causality identified from the gradients of the deep network.

The causal relationships discovered from the gradients of deep networks may include undirected edges, which to some extent represent the similarity between sequences. Our intuition is that this similarity should be equal in both directions. In fact, the widely used relationship matrices obtained from cosine similarity are symmetric matrices, thus assuming symmetry in both directions has convincing empirical evidence. Based on this intuition, we propose a simple and easy-to-use method for sparsifying causality graphs:

$$\begin{aligned} \tilde{A}_{i,j} &= \max(0, A_{i,j} - A_{i,j}^T), i \neq j, \\ \tilde{A}_{i,i} &= A_{i,i}. \end{aligned} \quad (6)$$

In which  $\tilde{A}$  is the sparsified Granger causality graph matrix. The causality matrix subtracted from its transpose eliminates bidirectional symmetric similarities while preserving unidirectional Granger causality. Further, we set a sparsity threshold  $h$ , setting causality effect values below this threshold in the causality graph matrix to zero. This is because insignificant causal relationships may be caused by noise and are not helpful for anomaly detection.

### Causal Deviation Scoring

By sliding a window over the test set and using the proposed framework to construct Granger causality graphs, we obtain a sequence of causality graphs. We aim to detect anomalies that deviate from the normal causal patterns within these graphs. A straightforward idea is to construct a causality graph that represents the normal causal pattern and compare each causality graph from the test set against it. To leverage the causal pattern information from the normal data, after model training, we sample the training set windows using a Bernoulli distribution and calculate the Granger causality graphs for these samples. Then, we use the mean matrix of the graph matrix sequence to represent the typical normal causal pattern:

$$\begin{aligned} W'_{train} &= W_{train} \odot B, \\ B &= \{b_1, \dots, b_{n_{train}}\}, \\ b_i &\sim \text{Bernoulli}(p), \\ A_{norm,i} &= \{g(W'_{train,i})\}_{i=1}^n, \end{aligned} \quad (7)$$

where  $n_{train}$  is the total number of sliding windows in the training set,  $p$  is the parameter of the Bernoulli distribution,  $n$  is the number of sampled windows, and  $g$  is the function used to compute the causality graph. The resulting typical

causality pattern matrix  $\bar{A}_{norm} \in \mathbb{R}^{N \times N}$ :

$$\bar{A}_{norm} = \frac{1}{n} \sum_{i=1}^n \tilde{A}_{norm,i}, \quad (8)$$

where  $\tilde{A}_{norm}$  is the sparsified causal matrix, and  $n$  is the total number of samples obtained through sampling.

Calculate the Granger causality graph for each window in the test set  $W_{test}$ :

$$\tilde{A}_{test} = \{g(W_{test,i})\}_{i=1}^n. \quad (9)$$

Define the causal deviation score for each test sample as:

$$Sc_i = \sum \frac{|\tilde{A}_{test,i} - \bar{A}_{norm}|}{\bar{A}_{norm} + \varepsilon}, \quad (10)$$

where  $\varepsilon$  is a very small value, and  $Sc$  represents the sequence of causal deviation scores. According to Equation 5, the main diagonal of the causality graph matrix represents the extent to which variables influence their own predicted values within the maximum time lag. To some extent, the values on the main diagonal reflect time-dependent patterns, although they do not explicitly provide the specifics of time dependence. We define the time pattern deviation as follows:

$$St_i = \sum \frac{|diag(\tilde{A}_{test,i} - \bar{A}_{norm})|}{diag(\bar{A}_{norm}) + \varepsilon}. \quad (11)$$

$St$  is the sequence of time pattern deviations, and  $diag(\cdot)$  refers to forming a diagonal matrix from the main diagonal elements. The final anomaly score is composed of a mixture of causal pattern deviations and time pattern deviations:

$$S = Sc + \beta St, \quad (12)$$

where  $\beta$  is a hyperparameter that balances the causal pattern deviation and the time pattern deviation. Note that the causal pattern deviation score inherently includes the main diagonal information, so even when  $\beta$  is set to 0, it still contains time pattern information.

## Experimental Results

To evaluate our proposed GCAD framework, we conducted experiments on five widely-used real-world benchmark datasets and compared it with six popular baseline methods.

### Experimental Setup

**Datasets.** Experiments are conducted on five real-world datasets, including SWaT (Mathur and Tippenhauer 2016), SMD (Su et al. 2019), MSL, SMAP (Hundman et al. 2018), and PSM (Abdulaal, Liu, and Lancewicki 2021). The statistical information of these datasets is presented in Table 1.

**Baseline Methods.** The baseline methods include DAGMM (Zong et al. 2018), USAD (Audibert et al. 2020), GDN (Deng and Hooi 2021), AnomalyTransformer(AT) (Xu et al. 2021), GANF (Dai and Chen 2022) and MEMTO (Song et al. 2024).

Dataset	channels	train	test	anomalies
SWaT	51	47,520	44,991	12.20%
SMD	38	28,479	28,479	9.46%
MSL	55	3,682	2,856	0.74%
SMAP	25	2,876	8,579	2.14%
PSM	25	132,481	87,841	27.76%

Table 1: Statistics of the Datasets

**Implementation Details.** Each dataset consists of two parts: unlabeled normal operation data and labeled data containing some anomalies. We use 80% of the normal data for training, and the remaining 20% is used for the validation set. Testing is conducted on the data containing anomalies. Since most baseline methods do not provide a way to set predetermined thresholds, we evaluate using two threshold-independent metrics: the Area Under the Curve (AUC) of the Receiver Operating Characteristic (ROC) and the Precision-Recall Curve (PRC). All experiments were conducted 10 times and the average results were reported.

### Anomaly Detection Performance

The results of our framework and the six baseline methods are summarized in Table 2.

From the results, it can be seen that GCAD achieves state-of-the-art (SOTA) performance in most cases. DAGMM and USAD are classical anomaly detection frameworks that do not explicitly model the spatial relationships between sequences, which limits their anomaly detection performance. GDN achieves the second-best performance across four experimental metrics; however, it uses an adaptive graph structure learning strategy to learn a fixed graph structure, which is not suitable for dynamically changing systems. GANF achieves the best result on the PRC metric for the SMAP dataset. This is because the SMAP dataset has severe distribution shifts, and GANF, being a density-based method, can better handle this situation by learning the evolution of graph structures and identifying distribution shifts. It is worth noting that the MSL and SMAP datasets are relatively small and have severe class imbalance, which may lead to very low PRC values for most methods. MEMTO, by incrementally training individual items in a gated memory module, mitigates the overgeneralization problem of reconstruction-based models. Therefore, it achieves the second-best result on the MSL dataset, where the proportion of anomalous samples is extremely small.

### Ablation Study

We investigated the effect of each component in the proposed framework. Table 3 shows the results of the ablation study on two datasets. ”-Spars” indicates the removal of the Causality Graph Sparsification part from GCAD. ”-GC” means not using Granger causality for anomaly detection. ”-TC” means disregarding the temporal correlations within each sequence by excluding the time pattern deviation from the anomaly score.

Dataset Metric	SWaT		SMD		MSL		SMAP		PSM	
	ROC	PRC	ROC	PRC	ROC	PRC	ROC	PRC	ROC	PRC
DAGMM	0.7882	0.4955	0.7516	0.3988	0.6209	0.0163	0.5989	0.0380	0.6556	0.3860
USAD	0.8318	<u>0.7173</u>	<u>0.9274</u>	0.5316	0.5601	0.0108	0.5314	0.0279	0.6584	0.4924
GDN	<u>0.8493</u>	<u>0.6076</u>	<u>0.9006</u>	<u>0.5655</u>	0.3846	0.0055	0.5115	0.0338	<u>0.7284</u>	<u>0.4964</u>
AT	0.5117	0.1851	0.1765	<u>0.0576</u>	0.5391	0.0141	0.3467	0.0188	<u>0.5058</u>	<u>0.2902</u>
GANF	0.8112	0.3557	0.6384	0.0017	0.6402	0.0291	<u>0.6926</u>	<b>0.5259</b>	0.6335	0.4090
MEMTO	0.7799	0.6067	0.5042	0.1187	<u>0.7271</u>	<u>0.0654</u>	0.4791	0.0176	0.5026	0.2913
GCAD	<b>0.8690</b>	<b>0.7758</b>	<b>0.9533</b>	<b>0.7502</b>	<b>0.7658</b>	<b>0.3679</b>	<b>0.7273</b>	<u>0.4555</u>	<b>0.7618</b>	<b>0.6136</b>

Table 2: Anomaly detection accuracy in terms of AUROC and AUPRC, on five benchmark datasets with ground-truth labelled anomalies

Dataset Metric	SWaT		SMD	
	ROC	PRC	ROC	PRC
GCAD	<b>0.8690</b>	<b>0.7758</b>	<b>0.9533</b>	<b>0.7502</b>
- Spars	0.8559	0.7676	0.9531	0.6915
- GC	0.8478	0.7513	0.9405	0.6424
- TC	0.8400	0.7558	0.9498	0.6748

Table 3: Ablation study. The anomaly detection results with and without components in GCAD

The results show that causal graph sparsification brings certain performance improvements. This is because sparsification helps mitigate the impact of sequence similarity on causal relationship discovery. Furthermore, data from large-scale systems typically consist of numerous channels. Sparsification helps reduce noise in the identified causal relationships.

The introduction of Granger causality and temporal correlations has led to significant performance improvements. This demonstrates that our model effectively captures the spatial and temporal associations in time series data. Overall, Granger causality more noticeably enhances our model’s performance, indicating that using causal relationships for anomaly detection in real-world datasets is important and effective.

### Effect of Parameters

We further investigated the impact of key hyperparameters on the anomaly detection performance of GCAD. All experiments were conducted using the SWaT dataset, and the results are shown in Figure 2.

The maximum time lag  $t$  determines how many lagged effects of Granger causality the model can discover. When  $t$  is set to 1, the model only discovers Granger causality in adjacent time steps, and the shorter sliding window makes the model more sensitive to anomalies within the window. As  $t$  increases, the model can discover Granger causality with higher lags, which helps extract more complex high-order spatial patterns. However, this also reduces the model’s sensitivity to short-term anomalies, because GCAD focuses on the causal patterns in the input distribution over the entire

window (Equation 5). Therefore, the maximum time lag parameter controls the balance between the model’s sensitivity to anomalies and its ability to discover complex anomalies. A moderate  $t$  value can achieve better performance.

The sparsification parameter  $h$  determines the threshold below which causal relationships are considered as noise. When  $h$  is small, there are many non-zero but insignificant causal relationships in the causality matrix. When  $h$  is too large, GCAD focuses only on the most significant causal relationships, ignoring the broader causal relationships that exist in the system, thus failing to fully utilize the anomaly information contained in the causal patterns. Experiments show that a moderate  $h$  can yield better results.

### Analysis of Anomaly Detection Examples

To demonstrate how causal patterns reveal anomalies, we conducted a case study on anomaly event data from a real system. The experiments were performed on the SWaT dataset, as the original authors (Goh et al. 2017) provided the physical construction and sensor descriptions of this real system.

To facilitate observation, we visualized the causal pattern deviations provided by GCAD during the occurrence of anomaly events, as shown in Figure 3. In this figure, the deviation matrix  $D$  represents the absolute error between the causality matrix during the anomaly event and the typical causality pattern matrix, that is,  $D = |\tilde{A}_{test,i} - \bar{A}_{norm}|$ .

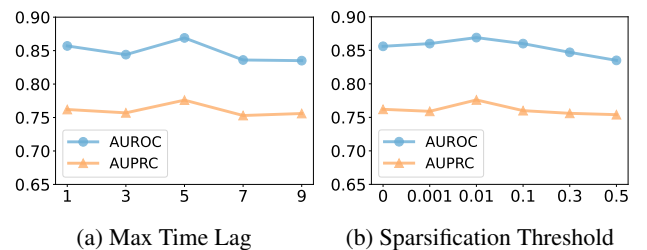


Figure 2: Effect of parameters. AUROC and AUPRC as functions of (a) maximum time lag  $\tau$  in Granger causality and (b) sparsification threshold  $h$  of the causal graph

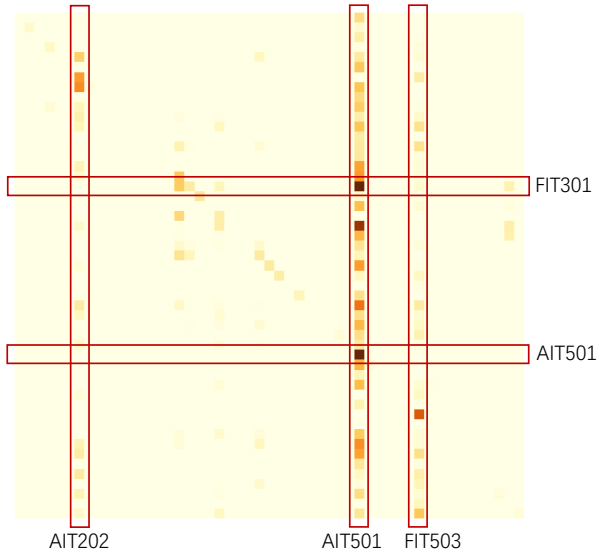


Figure 3: Causal Pattern Deviation Matrix in an Example Anomaly on the SWaT Dataset

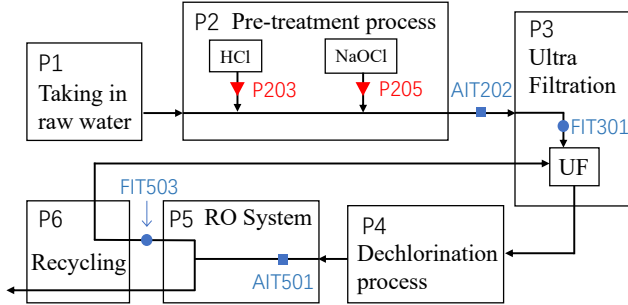


Figure 4: Physical Structure of the SWaT Testbed, Attack Points of Anomalous Events (marked in red), and Main Affected Points (marked in blue)

Darker colors indicate larger deviations. We have marked the main affected points in this attack in Figure 3, and Figure 4 illustrates the physical relationships between these points.

Specifically, this anomaly attack targeted P203 and P205, which are two pumps in Process 2 responsible for the addition of HCl and NaOCl, respectively. The attackers maliciously shut down these two pumps, causing changes in water quality. AIT202, located downstream of the attack points, is a sensor that measures the concentration of HCl in the water. The most significantly affected sensor is AIT501, located in Process 5 downstream, which is another sensor measuring HCl concentration. When the HCl injection pumps were attacked, the two sensors related to HCl exhibited significant deviations in their causal patterns, indicating that GCAD can effectively detect anomalous changes in causal patterns. Notably, the main diagonal element value corresponding to AIT501 is relatively large, which means AIT501 has a significant temporal pattern deviation for itself, highlighting the importance of incorporating temporal pattern deviations into

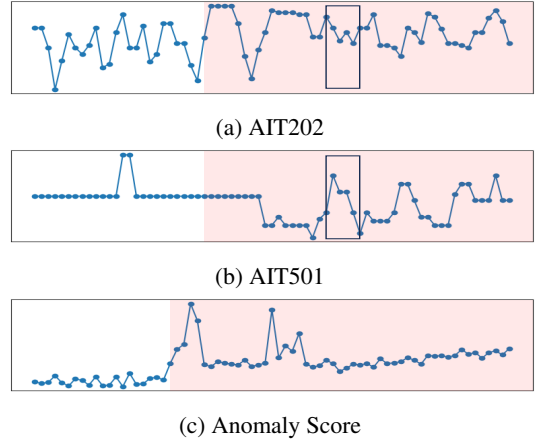


Figure 5: Two Affected Sensors and the Changes in the Total Anomaly Score in the Example Anomalous Instances

causal pattern deviations. The other two points with notable causal deviations are FIT301 and FIT503, which are flow meters. FIT301 measures the input flow to the UF module, and FIT503 measures the RO Reject flow. The deviations at these two points arise from changes in the relationships between certain flows and other sensors in the system under attack.

Figure 5 shows the changes in the two sensors measuring HCl concentration and the variations in anomaly scores during the attack. The red areas indicate the presence of anomaly events, and the causality matrix is derived from the marked sliding window. It can be observed that anomalies in a single sequence are difficult to identify manually. This is because real-world systems like SWaT have complex system dynamics and control logic, where anomalous events may not cause significant fluctuations in the time series. However, GCAD captures the causal relationships between sequences and provides significant changes in anomaly scores by detecting deviations in Granger causal patterns.

## Conclusion

In this work, we propose a Granger Causality-based multivariate time series Anomaly Detection method (GCAD). This framework models the spatial dependencies between sequences using Granger causality, constructs dynamic causal relationships based on the gradients of a deep predictor, and improves the causal graph structure using our sparsification strategy. Experiments on five real-world sensor datasets demonstrate the superiority of GCAD in anomaly detection accuracy compared to other baseline methods. This study explores the integration of Granger causality with deep networks, offering a new perspective for time series anomaly detection. However, GCAD also has some limitations, as it can only capture binary causal pairs between variables and cannot model multivariable interactions. Future work may consider multivariable causal relationships to uncover more complex anomalies.

## Acknowledgments

This work was supported in part by the Zhejiang Provincial Natural Science Foundation of China under Grant LDT23F01012F01, in part by the Zhejiang Provincial Natural Science Foundation under Grant MS25F030032 and in part by the National Natural Science Foundation of China under Grants 62372146 and 62003120.

## References

- Abdulaal, A.; Liu, Z.; and Lancewicki, T. 2021. Practical approach to asynchronous multivariate time series anomaly detection and localization. In *Proceedings of the 27th ACM SIGKDD conference on knowledge discovery & data mining*, 2485–2494.
- Audibert, J.; Michiardi, P.; Guyard, F.; Marti, S.; and Zuluaga, M. A. 2020. Usad: Unsupervised anomaly detection on multivariate time series. In *Proceedings of the 26th ACM SIGKDD international conference on knowledge discovery & data mining*, 3395–3404.
- Chen, S.-A.; Li, C.-L.; Arik, S. O.; Yoder, N. C.; and Pfister, T. 2023. TSMixer: An All-MLP Architecture for Time Series Forecasting. *Transactions on Machine Learning Research*.
- Chen, W.; Tian, L.; Chen, B.; Dai, L.; Duan, Z.; and Zhou, M. 2022. Deep variational graph convolutional recurrent network for multivariate time series anomaly detection. In *International conference on machine learning*, 3621–3633.
- Chen, Z.; Chen, D.; Zhang, X.; Yuan, Z.; and Cheng, X. 2021. Learning graph structures with transformer for multivariate time-series anomaly detection in IoT. *IEEE Internet of Things Journal*, 9(12): 9179–9189.
- Cheng, Y.; Wang, Z.; Xiao, T.; Zhong, Q.; Suo, J.; and He, K. 2024. CausalTime: Realistically Generated Time-series for Benchmarking of Causal Discovery. In *The Twelfth International Conference on Learning Representations*.
- Cheng, Y.; Yang, R.; Xiao, T.; Li, Z.; Suo, J.; He, K.; and Dai, Q. 2022. CUTS: Neural Causal Discovery from Irregular Time-Series Data. In *The Eleventh International Conference on Learning Representations*.
- Dai, E.; and Chen, J. 2022. Graph-augmented normalizing flows for anomaly detection of multiple time series. In *International Conference on Learning Representations*.
- Deng, A.; and Hooi, B. 2021. Graph neural network-based anomaly detection in multivariate time series. In *Proceedings of the AAAI conference on artificial intelligence*, volume 35, 4027–4035.
- Goh, J.; Adepu, S.; Junejo, K. N.; and Mathur, A. 2017. A dataset to support research in the design of secure water treatment systems. In *Critical Information Infrastructures Security: 11th International Conference, CRITIS 2016, Paris, France, October 10–12, 2016, Revised Selected Papers 11*, 88–99. Springer.
- Granger, C. W. 1969. Investigating causal relations by econometric models and cross-spectral methods. *Econometrica: journal of the Econometric Society*, 424–438.
- Han, S.; and Woo, S. S. 2022. Learning sparse latent graph representations for anomaly detection in multivariate time series. In *Proceedings of the 28th ACM SIGKDD Conference on Knowledge Discovery and Data Mining*, 2977–2986.
- Hundman, K.; Constantinou, V.; Laporte, C.; Colwell, I.; and Soderstrom, T. 2018. Detecting spacecraft anomalies using lstms and nonparametric dynamic thresholding. In *Proceedings of the 24th ACM SIGKDD international conference on knowledge discovery & data mining*, 387–395.
- Jin, M.; Koh, H. Y.; Wen, Q.; Zambon, D.; Alippi, C.; Webb, G. I.; King, I.; and Pan, S. 2024. A survey on graph neural networks for time series: Forecasting, classification, imputation, and anomaly detection. *IEEE Transactions on Pattern Analysis and Machine Intelligence*.
- Keogh, E.; Lin, J.; and Fu, A. 2005. Hot sax: Efficiently finding the most unusual time series subsequence. In *Fifth IEEE International Conference on Data Mining (ICDM'05)*, 8–pp. Ieee.
- Khanna, S.; and Tan, V. Y. 2019. Economy Statistical Recurrent Units For Inferring Nonlinear Granger Causality. In *International Conference on Learning Representations*.
- Li, D.; Chen, D.; Jin, B.; Shi, L.; Goh, J.; and Ng, S.-K. 2019. MAD-GAN: Multivariate anomaly detection for time series data with generative adversarial networks. In *International conference on artificial neural networks*, 703–716. Springer.
- Li, Z.; Zhao, Y.; Han, J.; Su, Y.; Jiao, R.; Wen, X.; and Pei, D. 2021. Multivariate time series anomaly detection and interpretation using hierarchical inter-metric and temporal embedding. In *Proceedings of the 27th ACM SIGKDD conference on knowledge discovery & data mining*, 3220–3230.
- Liu, M.; Sun, X.; Hu, L.; and Wang, Y. 2023. Causal discovery from subsampled time series with proxy variables. *Advances in neural information processing systems*, 36.
- Mathur, A. P.; and Tippenhauer, N. O. 2016. SWaT: A water treatment testbed for research and training on ICS security. In *2016 international workshop on cyber-physical systems for smart water networks (CySWater)*, 31–36. IEEE.
- Munir, M.; Siddiqui, S. A.; Dengel, A.; and Ahmed, S. 2018. DeepAnT: A deep learning approach for unsupervised anomaly detection in time series. *Ieee Access*, 7: 1991–2005.
- Park, D.; Hoshi, Y.; and Kemp, C. C. 2018. A multimodal anomaly detector for robot-assisted feeding using an lstm-based variational autoencoder. *IEEE Robotics and Automation Letters*, 3(3): 1544–1551.
- Qiu, H.; Liu, Y.; Subrahmanya, N. A.; and Li, W. 2012. Granger causality for time-series anomaly detection. In *2012 IEEE 12th international conference on data mining*, 1074–1079. IEEE.
- Shojaie, A.; and Fox, E. B. 2022. Granger causality: A review and recent advances. *Annual Review of Statistics and Its Application*, 9: 289–319.
- Song, J.; Kim, K.; Oh, J.; and Cho, S. 2024. Memto: Memory-guided transformer for multivariate time series anomaly detection. *Advances in Neural Information Processing Systems*, 36.



- Su, Y.; Zhao, Y.; Niu, C.; Liu, R.; Sun, W.; and Pei, D. 2019. Robust anomaly detection for multivariate time series through stochastic recurrent neural network. In *Proceedings of the 25th ACM SIGKDD international conference on knowledge discovery & data mining*, 2828–2837.
- Tank, A.; Covert, I.; Foti, N.; Shojaie, A.; and Fox, E. B. 2021. Neural granger causality. *IEEE Transactions on Pattern Analysis and Machine Intelligence*, 44(8): 4267–4279.
- Tayeh, T.; Aburakhia, S.; Myers, R.; and Shami, A. 2022. An attention-based ConvLSTM autoencoder with dynamic thresholding for unsupervised anomaly detection in multivariate time series. *Machine Learning and Knowledge Extraction*, 4(2): 350–370.
- Tuli, S.; Casale, G.; and Jennings, N. R. 2022. TranAD: Deep Transformer Networks for Anomaly Detection in Multivariate Time Series Data. *Proceedings of VLDB*, 15(6): 1201–1214.
- Wang, X.; Lin, J.; Patel, N.; and Braun, M. 2018. Exact variable-length anomaly detection algorithm for univariate and multivariate time series. *Data Mining and Knowledge Discovery*, 32: 1806–1844.
- Xu, J.; Wu, H.; Wang, J.; and Long, M. 2021. Anomaly Transformer: Time Series Anomaly Detection with Association Discrepancy. In *International Conference on Learning Representations*.
- Yu, Q.; Jibin, L.; and Jiang, L. 2016. An improved ARIMA-based traffic anomaly detection algorithm for wireless sensor networks. *International Journal of Distributed Sensor Networks*, 12(1): 9653230.
- Zamanzadeh Darban, Z.; Webb, G. I.; Pan, S.; Aggarwal, C.; and Salehi, M. 2024. Deep learning for time series anomaly detection: A survey. *ACM Computing Surveys*, 57(1): 1–42.
- Zhang, C.; Song, D.; Chen, Y.; Feng, X.; Lumezanu, C.; Cheng, W.; Ni, J.; Zong, B.; Chen, H.; and Chawla, N. V. 2019. A deep neural network for unsupervised anomaly detection and diagnosis in multivariate time series data. In *Proceedings of the AAAI conference on artificial intelligence*, volume 33, 1409–1416.
- Zhang, W.; Zhang, C.; and Tsung, F. 2022. GRELEN: Multivariate Time Series Anomaly Detection from the Perspective of Graph Relational Learning. In *International Joint Conference on Artificial Intelligence*, 2390–2397.
- Zhang, X.; Jiao, P.; Gao, M.; Li, T.; Wu, Y.; Wu, H.; and Zhao, Z. 2024. VGGM: Variational Graph Gaussian Mixture Model for Unsupervised Change Point Detection in Dynamic Networks. *IEEE Transactions on Information Forensics and Security*.
- Zhang, Z.; Geng, Z.; and Han, Y. 2024. Graph Structure Change-Based Anomaly Detection in Multivariate Time Series of Industrial Processes. *IEEE Transactions on Industrial Informatics*.
- Zheng, Y.; Koh, H. Y.; Jin, M.; Chi, L.; Phan, K. T.; Pan, S.; Chen, Y.-P. P.; and Xiang, W. 2023. Correlation-aware spatial-temporal graph learning for multivariate time-series anomaly detection. *IEEE Transactions on Neural Networks and Learning Systems*.
- Zhou, B.; Liu, S.; Hooi, B.; Cheng, X.; and Ye, J. 2019. Beatgan: Anomalous rhythm detection using adversarially generated time series. In *International Joint Conference on Artificial Intelligence*, volume 2019, 4433–4439.
- Zong, B.; Song, Q.; Min, M. R.; Cheng, W.; Lumezanu, C.; Cho, D.; and Chen, H. 2018. Deep autoencoding gaussian mixture model for unsupervised anomaly detection. In *International conference on learning representations*.